

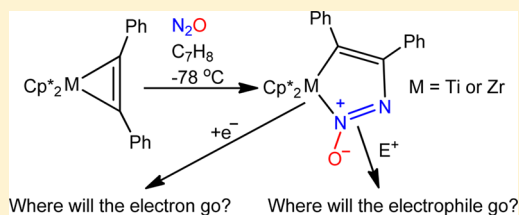
Functionalization of Complexed N₂O in Bis(pentamethylcyclopentadienyl) Systems of Zirconium and Titanium

Daniel J. Mindiola,^{*,†} Lori A. Watson,[‡] Karsten Meyer,[§] and Gregory L. Hillhouse[⊥]

Searle Chemistry Laboratory, Department of Chemistry, The University of Chicago, Chicago, Illinois 60637, United States

S Supporting Information

ABSTRACT: Methyl triflate reacts with the metastable azoxymetallacyclopentene complex Cp^{*}₂Zr(N(O)NCPPhCPh), generated *in situ* from nitrous oxide insertion into the Zr–C bond of Cp^{*}₂Zr(η²-PhCCPh) at –78 °C, to afford the salt [Cp^{*}₂Zr(N(O)N(Me)CPhCPh)][O₃SCF₃] (**1**) in 48% isolated yield. A single-crystal X-ray structure of **1** features a planar azoxymetallacycle with methyl alkylation taking place only at the β-nitrogen position of the former Zr(N(O)NCPPhCPh) scaffold. In addition to **1**, the methoxy-triflate complex Cp^{*}₂Zr(OMe)(O₃SCF₃) (**2**) was also isolated from the reaction mixture in 26% yield and fully characterized, including its independent synthesis from the alkylation of Cp^{*}₂Zr=O(NC₅H₅) with MeO₃SCF₃. Complex **2** could also be observed, spectroscopically, from the thermolysis of **1** (80 °C, 2 days). In contrast to Cp^{*}₂Zr(N(O)NPhCCPh), the more stable titanium N₂O-inserted analogue, Cp^{*}₂Ti(N(O)NCPPhCPh), reacts with MeO₃SCF₃ to afford a 1:1 mixture of regioisomeric salts, [Cp^{*}₂Ti(N(O)N(Me)CPhCPh)][O₃SCF₃] (**3**) and [Cp^{*}₂Ti(N(OMe)NCPPhCPh)][O₃SCF₃] (**4**), in a combined 65% isolated yield. Single-crystal X-ray diffraction studies of a cocrystal of **3** and **4** show a 1:1 mixture of azoxymetallacycle salts resulting from methyl alkylation at both the β-nitrogen and the β-oxygen of the former Ti(N(O)NCPPhCPh) ring. As opposed to alkylation reactions, the one-electron reduction of Cp^{*}₂Ti(N(O)NCPPhCPh) with K⁺, followed by encapsulation with the cryptand 2,2,2-Kryptofix, resulted in the isolation of the discrete radical anion [K(2,2,2-Kryptofix)][Cp^{*}₂Ti(N(O)NCPPhCPh)] (**5**) in 68% yield. Complex **5** was studied by single-crystal X-ray diffraction, and its solution X-band EPR spectrum suggested a nonbonding σ-type wedge hybrid orbital on titanium, d(z²)/d(x²–y²), houses the unpaired electron, without perturbing the azoxymetallacycle core in Cp^{*}₂Ti(N(O)NCPPhCPh). Theoretical studies of Ti and the Zr analogue are also presented and discussed.



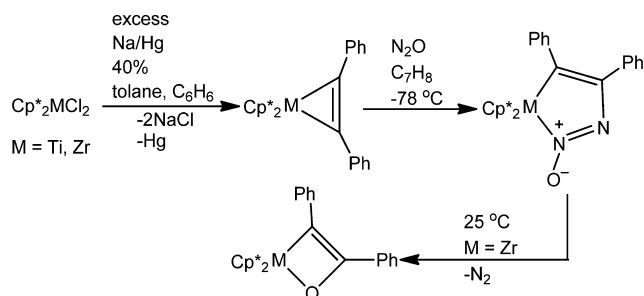
INTRODUCTION

Due to the thermodynamic oxidizing power of nitrous oxide ($\Delta G_f^\circ = 25$ kcal/mol) and its kinetic inertness in the absence of a suitable activating metal center, the development of systems capable of catalyzing the oxidation of organic or inorganic substrates using this greenhouse feedstock represents a paradigm in inorganic chemistry.^{1,2} Unlike most common powerful oxidants, nitrous oxide is cheap and very soluble in organic solvents such as toluene, alcohols, ethers, oils, water, and acids, with the advantage of such a chemical being resourceful, nonflammable, and essentially harmless. Therefore, it is not surprising that there has been considerable interest in employing N₂O for oxygen-atom transfer reactions.^{3–21} Unfortunately, and as noted before, this molecule is kinetically inert due to its poor properties as a ligand,^{22–24} consequently resulting in only a handful of systems being capable of complexing N₂O without the entropic and enthalpic driving force to N₂ ejection and metal oxo formation.^{11,12,18,22–31} Thus, the use of N₂O as an oxidizing substrate in transition metal chemistry is often hampered by a combination of kinetic inertness and inevitable oxidation of the metal center, concomitant with entropy-assisted loss of a thermodynamically stable molecule such as dinitrogen.³²

Given the disposition of nitrous oxide as being a poor ligand in the realm of coordination chemistry, our group and others are pursuing the use of nitrous oxide in O atom transfer systems for the purpose of oxidation catalysis. Previously, we reported that group 4 transition metals (Ti and Zr) can insert nitrous oxide into a strained M–C bond without oxidation of the metal center to form bis(pentamethylcyclopentadienyl) systems, having coordinated N₂O as part of the ligand scaffold (Scheme 1).^{11,12} As a result, N₂O functionalizes the ligand (e.g., toluene) *without immediate extrusion* of N₂. Although N₂ extrusion can in one case occur, affording an oxametallacycle, this process depends heavily on the metal in question (zirconium vs titanium, Scheme 1).¹² The fact that the azoxymetallacycle complex Cp^{*}₂Ti(N(O)NCPPhCPh)^{11,12,33} was not prone to dinitrogen elimination under ambient conditions (unlike its Zr derivative), to give a hypothetical oxametallacyclobutene system Cp^{*}₂Ti(OCPhCPh), led us to speculate that such a system could be ideal for O atom and/or functionalization reactions stemming from N₂O complexation (Scheme 1).¹¹ In addition, the azoxymetallacyclobutene moiety in complexes of the type Cp^{*}₂M(N(O)NCPPhCPh) (M = Ti or

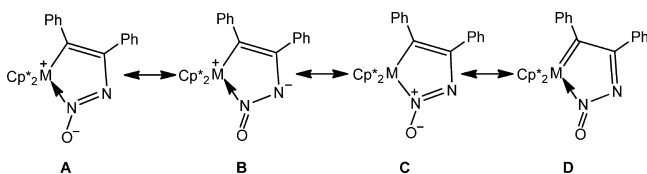
Received: March 10, 2014

Scheme 1. Nitrous Oxide Insertion into a Strained Metal–Carbon Bond of an η^2 -Tolene Bis(pentamethylcyclopentadienyl) Complex and N_2 Extrusion to Form an Oxymetallacyclobutene



Zr) provides an ideal opportunity to examine the charge distribution about this rare functionality since several canonical forms can be envisioned (Scheme 2). While resonance

Scheme 2. Proposed Canonical Forms for the Azoxymetallacyclobutene Framework in Complexes of the Type $Cp^*_2M(N(O)NCPPhCPh)$ ($M = Ti$ and Zr)



structures **A** and **B** represent zwitterionic forms with negative charge being localized on β -O and the β -N, respectively, resonance form **C** can be best represented as an ylide, having more nucleophilic character on O (Scheme 2). Another probable form in $Cp^*_2M(N(O)NCPPhCPh)$ is the formation of an *N*-nitroso ketimine tethered alkylidene moiety, resonance **D**, where most of the nucleophilic charge is presumed to reside at the hindered alkylidene carbon (Scheme 2). Hence, examining the reactivity of $Cp^*_2M(N(O)NCPPhCPh)$ with an electrophile could provide some clues as to which site is likely most nucleophilic, but also allow us to further functionalize the $N(O)N$ motif resulting from N_2O insertion into a strained $M-C$ bond. Surprisingly, examples of homogeneous catalytic oxidation reactions using N_2O as an O atom transfer reagent are exceedingly rare, and examples include the oxidation with N_2O of PPh_3 using a cobalt(I) complex¹⁷ and the oxidation of styrene by a ruthenium porphyrin system.¹⁶ Unfortunately, the latter reaction has yet to be developed into an efficient catalytic cycle. This lackluster situation in homogeneous catalysis is rather unanticipated given the popular usage of N_2O in heterogeneous catalytic reactions such as the oxidation of benzene to phenol over supported metals³⁴ or Fe and Ru/ZSM-5 zeolites³⁵ and the oxidation of methane on silicomolybdate catalyst.³⁶

Herein, we report comparative studies of the reaction of an electrophile, such as MeO_3SCF_3 , with the azoxymetallacyclobutene scaffold in the compounds $Cp^*_2M(N(O)NCPPhCPh)$ ($M = Ti$ or Zr). Thermostability of the salt and the fate of coordination of the methyl cation were found to be highly dependent on the nature of the metal. In addition, it was also observed that the azoxymetallacyclobutene scaffold of complex $Cp^*_2Ti(N(O)NCPPhCPh)$ can be resistant to reducing conditions and house one unpaired electron, in the form of

the radical anion titanium(III) species $[Cp^*_2Ti(N(O)NCPPhCPh)]^-$, without significant perturbation of the azoxymetallacyclobutene core.

EXPERIMENTAL SECTION

General Considerations. Unless stated otherwise, all operations were performed in an M. Braun Lab Master drybox under an atmosphere of purified nitrogen or using high-vacuum and standard Schlenk techniques under an argon atmosphere.³⁷ HPLC grade or anhydrous solvents such as benzene, toluene, diethyl ether, *n*-hexane, pentane, and CH_2Cl_2 were purchased from Acros Chemicals or EM Science and were further dried by passage through activated alumina and/or Q-5 columns. THF was distilled from purple benzophenone ketyl solution under an inert atmosphere. C_6D_6 , $THF-d_8$, and CD_2Cl_2 were purchased from Cambridge Isotope Laboratory (CIL), degassed and dried over activated 4 Å molecular sieves. Celite, alumina, and 4 Å molecular sieves were activated *in vacuo* overnight at 180 °C. $Cp^*_2TiCl_2$ was prepared according to the literature³⁸ or purchased from Strem Chemicals and used as received. KC_8 ,³⁹ $Cp^*_2ZrCl_2$,⁴⁰ $Cp^*_2Zr(PhCCPh)$,³⁸ $Cp^*_2Ti(N(O)NCPPhCPh)$,¹¹ $Cp^*_2Zr(N(O)NCPPhCPh)$,^{11,12} $Cp^*_2Zr(OCPhCPh)$,¹² and $Cp^*_2Zr(O)(NC_3H_5)$ ^{15c} were prepared according to literature methods. $Cp^*_2Ti(PhCCPh)$ was prepared in 68% yield by a modified procedure from that reported in the literature, via reduction of $Cp^*_2TiCl_2$ with Na/Hg, and in the presence of $PhCCPh$, using a protocol identical to that reported for the zirconium derivative $Cp^*_2Zr(PhCCPh)$.³⁸ 2,2-Kryptofix was purchased from Aldrich and was dried by dissolving in a minimum of dry THF, then filtered through activated alumina, and the filtrate was dried under vacuum to afford a white powder. All other chemicals were used as received. Elemental analysis was performed by Desert Analytics (Tucson, AZ, USA). 1H , ^{13}C , and ^{19}F NMR spectra were recorded on Bruker 500 and 400 MHz NMR spectrometers. 1H and ^{13}C NMR spectra are reported with reference to solvent resonances (residual C_6D_5H in C_6D_6 , 7.16 and 128.0 ppm; residual H in CD_2Cl_2 , 5.32 and 53.8 ppm; residual H in $THF-d_8$, 1.73 and 3.58 ppm, and 65.6 and 23.5 ppm). ^{19}F NMR spectra are reported with respect to external CCl_3F (0.0 ppm). Room-temperature solution (THF) magnetic susceptibility measurements were determined by 1H NMR spectroscopy using the method of Evans.^{41,42} The room-temperature X-band EPR spectra were recorded on a Bruker EMX spectrometer. Acquisition, simulation, and data postprocessing of the solution spectra were performed using an integrated WIN-EPR software package (Bruker). Cyclic voltammetry measurements were collected with the assistance of an Eco-Chemie Autolab potentiostat (pgstat20) and the GPES 2.0 software from Bioanalytical Systems (BAS). X-ray diffraction data were collected on a Siemens Platform goniometer with a charged coupled device (Smart Apex). Structures were solved by direct or Patterson methods using the SHELXTL (version 5.1) program library (G. Sheldrick, Bruker Analytical X-ray Systems, Madison, WI, USA).⁴³

Preparation of $[Cp^*_2Zr(N(O)N(Me)CPhCPh)][O_3SCF_3]$ (1**).** Toluene (ca. 20 mL) was vacuum transferred into a Schlenk flask equipped with a stir bar and $Cp^*_2Zr(\eta^2-PhCCPh)$ [554 mg, 1.027 mmol]. The solution was placed under an N_2O atmosphere at -78 °C, causing a rapid color change from green-brown to orange. The orange solution was stirred under an atmosphere of N_2O at -78 °C for 1 h and then degassed. To the orange solution was added via cannula a similarly cold (-78 °C) toluene solution (ca. 8 mL) of MeO_3SCF_3 [171 mg, 1.042 mmol] under an argon atmosphere. The mixture was allowed to stir for 2 h at -78 °C, and the mixture was then slowly warmed to -42 °C and stirred for an additional 0.5 h, upon which an orange microcrystalline solid was observed to precipitate. Slow warming of the solution to room temperature afforded a yellow-orange solution with an orange precipitate. The reaction mixture was transferred into the glovebox and cooled to -35 °C. The cold solution was then filtered to remove the orange crystalline solid, which was washed with cold toluene followed by cold pentane. The solid was dried under vacuum to afford pure **1** [373 mg, 0.499 mmol, 48% yield in one crop]. 1H NMR (22 °C, 500.1 MHz, CD_2Cl_2): δ 1.57 (s,

$C_5(CH_3)_5$, 30 H), 3.05 (s, NCH_3 , 3 H), 5.32 (d, *o*-Ph, 2 H), 6.75 (m, Ph, 3 H), 7.08 (m, Ph, 2 H), 7.24 (m, Ph, 3 H). ^{13}C NMR (22 °C, CD_2Cl_2): δ 11.91 (q, $C_5(CH_3)_5$), 37.20 (q, NCH_3), 127.3 (s, $C_5(CH_3)_5$), 128.3, 128.8, 130.4, 130.5, 130.7, 133.4 (s), 137.5 (s), 190.8 (s). ^{19}F NMR (22 °C, 470.6 MHz, CD_2Cl_2): δ -81.7 (s, O_3SCF_3). Anal. Calcd for $C_{36}H_{43}F_3N_2O_4SZr$: C, 57.81; H, 5.79; N, 3.74. Found: C, 56.87; H, 5.65; N, 3.70. Complex 1 is thermally unstable in solution and must be stored as a solid at -35 °C.

Preparation of $Cp^*_2Zr(OMe)(O_3SCF_3)$ (2). Method A. The analogous procedure and scale reported for 1 was followed, and after separation of the toluene insoluble salt, 1, the filtrate was dried under vacuum and extracted with pentane, the solution filtered through Celite, the filtrate concentrated to ~2 mL, and then the solution cooled to -35 °C for 3–4 days under N_2 . The yellow solid was collected via filtration and dried under vacuum to afford pure 2 as evidenced by 1H NMR spectroscopy [143 mg, 0.264 mmol, 26% yield in two crops]. Examination of the pentane filtrate (after separation of 2) revealed a mixture of free toluene (PhCCPh) along with compound 2, as well as some other minor intractable products. Complex 2 is highly soluble in hydrocarbon solvents, but analytically pure complex can be obtained from recrystallization of the solid from a saturated solution in diethyl ether at -35 °C over 5–6 days. 1H NMR (22 °C, 500.1 MHz, C_6D_6): δ 1.80 (s, $C_5(CH_3)_5$, 30 H), 4.03 (s, OCH_3 , 3 H). ^{13}C NMR (22 °C, 125.8 MHz, C_6D_6): δ 10.99 (q, $C_5(CH_3)_5$), 59.31 (q, OCH_3), 123.2 (s, $C_5(CH_3)_5$), 128.3 (q, O_3SCF_3). ^{19}F NMR (22 °C, 470.6 MHz, C_6D_6): δ -78.7 (s, O_3SCF_3). Anal. Calcd for $C_{22}H_{33}F_3O_4SZr$: C, 48.77; H, 6.14; N, 0.00. Found: C, 48.90; H, 6.03; N, <0.09.

Preparation of $Cp^*_2Zr(OMe)(O_3SCF_3)$ (2). Method B. In a vial loaded with a stir bar $Cp^*_2Zr(O)(NC_5H_5)$ [100 mg, 0.219 mmol] was partially dissolved in toluene (ca. 5 mL), and the suspension cooled to -35 °C. A cold toluene solution (-35 °C, ca. 5 mL) containing MeO_3SCF_3 [38 mg, 0.236 mmol] was added dropwise, and the brown-yellow mixture allowed to stir for 1 h. The volatiles were removed under reduced pressure, the yellow-brown residue was extracted with pentane and filtered through Celite, and the filtrate was dried under vacuum to afford pure 2 as a light yellow powder [106 mg, 0.196 mmol, 89% yield]. 1H NMR spectroscopy of the crude reaction mixture confirmed clean formation of 2 by comparison with authentic samples reported by method A.

Preparation of $[Cp^*_2Ti(N(OMe)NCPPhCPh)][O_3SCF_3]$ (3) and $[Cp^*_2Ti(N(O)N(Me)CPhCPh)][O_3SCF_3]$ (4). In a Schlenk flask equipped with a stir bar $Cp^*_2Ti(N(O)NCPPhCPh)$ [180 mg, 0.333 mmol] was dissolved in toluene (ca. 30 mL), and the orange solution was cooled to -78 °C. To the cold solution was added via cannula a solution of MeO_3SCF_3 [58 mg, 0.353 mmol] dissolved in cold toluene (ca. 10 mL, -78 °C), causing a rapid color change to yellow-brown followed by immediate formation of a brown oil. The reaction mixture was slowly warmed to room temperature, and the solution transferred into the glovebox. The yellow mother liquor was decanted with a pipet, and the brown oil rinsed with toluene (1–2 mL) followed by diethyl ether (3 mL) and then *n*-hexanes (2 \times 5 mL). The remaining oil was dried under reduced pressure, extracted with 2 mL of CH_2Cl_2 , and filtered through a small pad of Celite, and the filtrate was concentrated to ~1 mL. Subsequently, the solution was carefully layered with diethyl ether until a fine mist formed at the interface. Cooling the CH_2Cl_2 /Et₂O layered solution to -35 °C for 6 days afforded dark red-brown blocks. Decanting of the solution and washing of the crystals with 2–3 mL of Et₂O/pentane (1:1) afforded pure 3 and 4 in a 1:1 cocystal mixture, as evinced by 1H and ^{13}C NMR spectroscopy [160 mg, 0.227 mmol, 68% yield combined from two crops]. Note: The solution obtained after separating the crystals can be cooled further for several more days to afford a second crop of 3 and 4. 1H NMR (22 °C, 500.1 MHz, CD_2Cl_2): δ 7.56 (m, Ph), 7.47 (m, Ph), 7.37 (m, Ph), 7.04 (m, Ph), 6.91 (t, Ph), 6.02 (br s, Ph), 5.58 (d, Ph), 3.93 (s, OCH_3 , 3 H), 3.56 (s, NCH_3 , 3 H), 1.93 (s, $C_5(CH_3)_5$, 30 H), 1.90 (s, $C_5(CH_3)_5$, 30 H). ^{13}C NMR (22 °C, 125.8 MHz, CD_2Cl_2): δ 225.8 (s, Ti-C), 204.3 (s, Ti-C), 141.3, 140.2, 139.0, 138.2, 133.9, 131.8, 131.6, 131.3, 130.7 (br s, O_3SCF_3), 130.4 (m), 130.2, 129.7, 129.6, 129.4, 129.1, 128.9, 128.7, 128.0, 127.7, 60.0 (q, OCH_3),

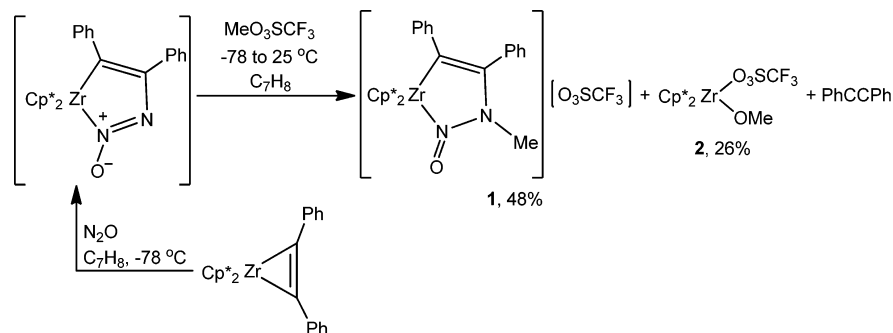
37.2 (q, NCH_3), 12.9 (q, $C_5(CH_3)_5$). ^{19}F NMR (22 °C, 470.6 MHz, CD_2Cl_2): δ -78.4 (s, O_3SCF_3). Anal. Calcd for $C_{36}H_{43}F_3N_2O_4STi$: C, 61.36; H, 6.15; N, 3.98. Found: C, 61.39; H, 6.21; N, 3.86.

Preparation of $[K(2,2,2\text{-Kryptofix})][Cp^*_2Ti(N(O)NCPPhCPh)]$ (5). In a 300 mL round-bottom flask under an N_2 atmosphere was dissolved $Cp^*_2Ti(N(O)NCPPhCPh)$ [278 mg, 0.515 mmol] in C_6H_6 (ca. 30 mL). To the orange-red solution was added in small portions freshly prepared KC_8 [77 mg, 0.570 mmol], causing an immediate color change of the solution to olive-green concomitant with generation of black graphite. After 20 min, the solution was filtered through a frit to remove the graphite and excess KC_8 . To the green filtrate was added, while stirring, a cold diethyl ether solution (ca. 5 mL, -35 °C) with dissolved 2,2,2-Kryptofix [193 mg, 0.513 mmol]. Upon complete addition of the cryptand, a small suspension was observed to form and the solution was allowed to stir for an additional 10 min. The solution was then concentrated to 10–15 mL to afford a green solid along with an oily residue. To this mixture was added a copious amount of pentane to induce precipitation of the green solid along with a green oil (cooling of the mixture also induces precipitation of green solids). The suspension-oily residue was then filtered through Celite, and the green solids were washed with a copious amount of pentane. The solids collected in the Celite were extracted with 8 mL of THF and filtered, and the filtrate was concentrated to ca. 6 mL. To the olive-green solution was added a few drops of pentane, causing formation of a mist at the solvent interface. To the misty solution was then added a few drops of diethyl ether to redissolve the mist. The solution was then cooled to -35 °C for 2 days. Dark green single crystals of 5 formed over this period, which were collected via filtration, washed with cold diethyl ether, and dried under vacuum [287 mg, 0.300 mmol, 58.3%]. Concentration of the filtrate after separation of the crystals and addition of excess diethyl ether, followed by cooling of the solution for 2 more days, afforded a second crop of crystals [46 mg, 0.0481 mmol, total yield combined 68%]. Mag. suscep. (Evans' method, THF, 298 K): $\mu_{eff} = 2.28 \mu_B$. EPR (THF, 295 K): $g_{iso} = 1.9846$, $A_{iso} (^{47}Ti, I = 5/2, 7.4\%) = 8.55 G$, $A_{iso} (^{14}N, I = 1, 99.64\%) = 2.0 G$, and $A_{iso} (^{14}N, I = 1, 99.64\%) = 0.5 G$. $\nu = 9.468$ GHz, MA = 0.5 G, MF = 100 kHz. 1H NMR (22 °C, 500.1 MHz, THF-*d*₈): δ 1.95 (m, crypt), 2.20 (br s), 2.73 (m, crypt), 3.78 (m, crypt), 7.50 (br s). Anal. Calcd for $C_{52}H_{74}O_7KTi$: C, 65.32; H, 8.01; N, 5.86. Found: C, 65.40; H, 8.24; N, 5.57.

Cyclic Voltammetry Measurements of $Cp^*_2Ti(N(O)NCPPhCPh)$. Cyclic voltammetry studies were performed in a predried solution of THF (0.3–0.8 M solution, containing predried and recrystallized tetrabutylammonium hexafluorophosphate, TBAH, Aldrich). A platinum disk (2.0 mm diameter, Bioanalytical Systems), a platinum wire, and a silver wire were employed as the working electrode, the auxiliary electrode, and the quasi-reference electrode, respectively. A one-cell compartment was used in the CV experiments. The electrochemical response was collected with the assistance of an Eco-Chemie Autolab potentiostat (pgstat20) and the Bioanalytical System (BAS) 100 W electrochemical workstation. All the potentials were reported against the ferrocenium/ferrocene couple (0 V) measured as an internal standard. All spectra were recorded at a scan rate of 100–200 mV/s under an N_2 atmosphere. In all instances, reversible waves were subjected to scan-rate dependence tests ranging from 20 to 1000 mV/s. In a typical experiment 8–14 mg of $Cp^*_2Ti(N(O)NCPPhCPh)$ were dissolved in a TBAH/THF solution at room temperature.

EPR Measurements of $[K(2,2,2\text{-Kryptofix})][Cp^*_2Ti(N(O)NCPPhCPh)]$ (5). The X-band EPR spectrum of 5 was recorded in THF at 298 K. Typical concentrations ranged from 0.05 to 10 mmol solutions in THF. The coupling constants were found by simulation to be $A_{iso} (^{47}Ti, I = 5/2, 7.4\%) = 8.55 G$, $A_{iso} (^{14}N, I = 1, 99.64\%) = 2.0 G$, and $A_{iso} (^{14}N, I = 1, 99.64\%) = 0.5 G$.

Crystal Structure Determinations. Data Collection and Structure Solution and Refinement. The crystal was mounted and centered on a Bruker SMART APEX system. The radiation used was Mo $K\alpha$ ($\lambda = 0.71073$ Å, $m = 4.413$ mm⁻¹). Rotation and still images showed diffractions to be sharp, while frames separated in reciprocal

Scheme 3. Alkylation of an Azoxymetallacyclobutene Complex with MeO_3SCF_3 to Afford **1** and **2**

space were obtained and provided an orientation matrix and initial cell parameters. Final cell parameters were obtained from the full data set. A “hemisphere” data set was obtained, which samples approximately 1.2 hemispheres of reciprocal space to a resolution of 0.84 \AA using 0.3° degree steps in ω and using 10 s interval times for each frame. Absorption corrections were applied using SADABS (references of all software and sources of scattering factors are contained in the SHELXTL (version 5.1) program library, G. Sheldrick, Bruker Analytical X-ray Systems, Madison, WI, USA). The space group was determined based on systematic absences and intensity statistics. Direct or Patterson methods were used to locate the heavy atoms, C atoms, and all other heteroatoms from the E-map. Repeated difference Fourier maps allowed recognition of all expected H atoms. Prior to location of H, other atoms were converted to and refined anisotropically. Hydrogen atoms were refined isotropically and were placed in calculated ($d_{\text{CH}} = 0.96 \text{ \AA}$) positions. Structures were collected at 100 K. Crystal data and structure analysis results are shown in the Supporting Information.

Crystal Structure of 1. An orange thin plate of **1** grown from slow evaporation of a CH_2Cl_2 solution was selected under a stereomicroscope while immersed in Paratone oil (Exxon) to avoid minimal contact with air. The crystal was removed from the oil using a tapered fiber, which also served to hold the crystal for data collection. The structure was solved by direct methods in conjunction with standard difference Fourier techniques. All non-hydrogen atoms were refined anisotropically, and hydrogens were placed in calculated positions. Two chemically equivalent but crystallographically independent molecules were confined in the asymmetric unit. No absorption correction was applied. The least-squares refinement converged normally.

Crystal Structure of 3 and 4. A dark red-brown block of **3** and **4** grown from a CH_2Cl_2 solution layered with Et_2O at -35°C was selected under a stereomicroscope while immersed in Paratone oil (Exxon) to avoid minimal contact with air. The crystal was removed from the oil using a tapered fiber, which also served to hold the crystal for data collection. The structure was solved by Patterson methods. Considerable electron density was confined next to O1. To account for this, the peak was selected as C1B and refined at nearly 1/2 occupancy with C1A. No anomalous bond lengths or thermal parameters were noted except for the methyl carbons C1a and C1b. Both atoms suffer from disorder and were fixed at approximately 0.52889 and 0.47111 occupancies using the second variable in the FVAR card, respectively. The thermal parameter was fixed for both atoms such that it would not change during refinement. Both C1a and C1b were refined anisotropically, but no hydrogens were placed at calculated positions for each of these atoms. All other non-hydrogen atoms were refined anisotropically, and hydrogens were placed in calculated positions. An absorption correction was applied in the refinement using semi-empirical methods from psi-scans (max. and min. transmission 0.8953 and 0.8639). The least-squares refinement converged normally. No extinction coefficient was applied.

Crystal Structure of Complex 5. A dark green block of **5** grown from a THF solution layered with a few drops of pentane/ Et_2O at -35°C was selected under a stereomicroscope while immersed in Paratone

oil (Exxon) to avoid minimal contact with air. The crystal was removed from the oil using a tapered fiber, which also served to hold the crystal for data collection. The structure was solved by direct methods in conjunction with standard difference Fourier techniques. All non-hydrogen atoms were refined anisotropically, and hydrogens were placed in calculated positions. No absorption correction was applied in the refinement. The least-squares refinement converged normally, and no extinction coefficient was applied.

Computational Details. All calculations were performed with the Gaussian 09 package⁴⁴ at the B3PW91⁴⁵ level of theory. Basis sets used included LANL2DZ for Ti and Zr and 6-31G(d) for H, C, N, and O.⁴⁶ The basis set LANL2DZ is the Los Alamos National Laboratory ECP plus a double- ζ valence on Ti/Zr.⁴⁷ All optimizations were performed with C_1 symmetry, and all minima were confirmed by analytical calculation of frequencies, which were also used to compute zero point energy corrections without scaling. The initial geometry of $\text{Cp}_2\text{Ti}(\text{N}(\text{O})\text{NCMeCMe})$ and $\text{Cp}_2\text{Zr}(\text{N}(\text{O})\text{NCMeCMe})$ was adapted from a refined crystal structure of $(\text{Cp}^*)_2\text{Ti}(\text{N}(\text{O})\text{NCPhCPh})$ ¹¹ with all methyl groups on the Cp^* replaced with H and phenyl groups on the metallacycle replaced by methyls.

RESULTS AND DISCUSSION

Reaction of $\text{Zr}(\text{N}(\text{O})\text{NCPhCPh})$ and $\text{Cp}^*_2\text{Zr}(\text{O})(\text{NC}_5\text{H}_4)$ with MeOTf. As reported in earlier work,^{11,12} treatment of a toluene solution of $\text{Cp}^*_2\text{Zr}(\eta^2\text{-PhCCPh})$ with N_2O at -78°C results in insertion of nitrous oxide into the $\text{Zr}-\text{C}(\text{alkyne})$ bond to afford the orange and thermally unstable complex $\text{Cp}^*_2\text{Zr}(\text{N}(\text{O})\text{NCPhCPh})$, which was not characterized.¹¹ Upon generation of metastable $\text{Cp}^*_2\text{Zr}(\text{N}(\text{O})\text{NCPhCPh})$, we found that addition of a cold toluene solution of MeO_3SCF_3 (-78°C) rapidly results in formation of the orange salt $[\text{Cp}^*_2\text{Zr}(\text{N}(\text{O})\text{N}(\text{Me})\text{CPhCPh})][\text{O}_3\text{SCF}_3]$ (**1**) in 48% isolated yield (Scheme 3). The ionic nature of **1** allows for facile separation from the reaction mixture, and, unlike its predecessor $\text{Cp}^*_2\text{Zr}(\text{N}(\text{O})\text{NCPhCPh})$, compound **1** is relatively stable as a solid when stored at -35°C . The most salient spectroscopic feature associated with **1** is the observation of a singlet in the ^1H NMR spectrum at 3.05 ppm, which corresponds to the methyl resonance derived from addition of the electrophile to the $\text{N}(\text{O})\text{N}$ motif. Complex **1** also exhibits a singlet at 1.57 ppm for the methyl protons of the ancillary Cp^* as well as multiplets ranging from 5.3 to 7.3 ppm, arising from the two inequivalent phenyl groups (10 hydrogens total). The insoluble nature of **1** in nonprotic and nonpolar solvents such as pentane, ether, and arenes suggests this system to be a discrete salt, while the ^{19}F NMR spectrum also implies a OTf^- counterion to be present in this species (-81.7 ppm).

The canonical forms, which are possible in the azoxymetallacyclobutene moiety in $\text{Cp}^*_2\text{Zr}(\text{N}(\text{O})\text{NPhCCPh})$ (*vide supra*, Scheme 2), suggest the $\beta\text{-O}$ and $\beta\text{-N}$ atoms to be the most exposed nucleophilic sites. In order to unambiguously

address the site of alkylation, a single-crystal X-ray diffraction study was undertaken. Accordingly, a single crystal was grown, and the molecular structure of **1** is shown in Figure 1,

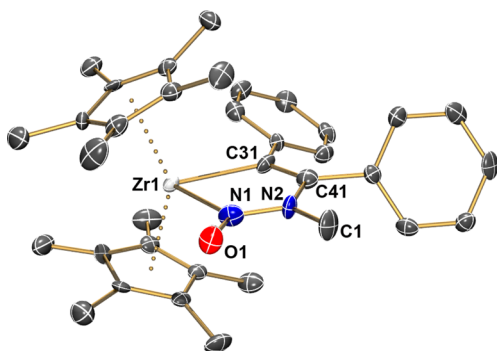


Figure 1. Perspective view of the molecular structure of only the cation component in complex **1** (and one crystallographically independent molecule), depicting the atom-labeling ellipsoid plot at the 50% probability level. H atoms have been omitted for clarity purposes.

illustrating one of the two chemically equivalent, but crystallographically independent molecules in the asymmetric unit. One interesting feature associated with the molecular structure of **1** is the retention of an azoxymetallacyclobutene ring in $\text{Cp}^*_2\text{Zr}(\text{N}(\text{O})\text{NPhCCPh})$, a previously reported unstable complex that eluded crystallographic analysis due to its propensity to eject N_2 and subsequently form the oxy-metallacyclobutene compound (Scheme 1).¹² In addition, the solid-state structure confirms methylation of the β -N position of the metallacycle ($\text{N}(2)-\text{C}(1)$, 1.457(8) Å). For comparison, the $\text{N}(1)-\text{N}(2)$ distance of 1.318(7) Å in the azoxymetallacycle fragment is relatively elongated from that of the titanium and neutral analogue, $\text{Cp}^*_2\text{Ti}(\text{N}(\text{O})\text{NCPHCPH})$.¹¹ Likewise, the $\text{N}-\text{O}$ distance is shorter than in $\text{Cp}^*_2\text{Ti}(\text{N}(\text{O})\text{NCPHCPH})$, implying a canonical structure such as the one depicted in Scheme 3. The metrical parameters of **1** are overall consistent with an approximately planar five-membered metallacycle (Table 2) with a long $\text{N}-\text{N}$ bond when compared to the

Table 2. Selected Bond Lengths (Å) and Dihedral Angles (deg) for Complex **1**

$\text{Zr}(1)-\text{N}(1)$	2.262(5)
$\text{Zr}(1)-\text{C}(31)$	2.309(6)
$\text{N}(1)-\text{O}(1)$	1.256(6)
$\text{N}(1)-\text{N}(2)$	1.318(7)
$\text{N}(2)-\text{C}(1)$	1.457(8)
$\text{N}(2)-\text{C}(41)$	1.458(8)
$\text{Zr}(1)-\text{N}(1)-\text{N}(2)-\text{C}(41)$	−2.2(6)
$\text{N}(1)-\text{N}(2)-\text{C}(41)-\text{C}(31)$	2.1(7)
$\text{Zr}(1)-\text{C}(31)-\text{C}(41)-\text{N}(2)$	−1.0(7)

similar functional group in *p*-azoxyanisole, $p\text{-MeOC}_6\text{H}_4\text{N}(\text{O})=\text{NC}_6\text{H}_4\text{-}p\text{-OMe}$ ($\text{N}-\text{N}$ = 1.218(5) Å).³³ As a result, complex **1** could also possess canonical forms **A** and **C**, as shown in Scheme 2, thereby forming a salt by positive charge at the β -nitrogen atom. The trapping and isolation of a discrete salt, **1**, undoubtedly implies that the thermally unstable intermediate $\text{Cp}^*_2\text{Zr}(\text{N}(\text{O})\text{NCPHCPH})$ must be the species reacting with the electrophile, since such an intermediate

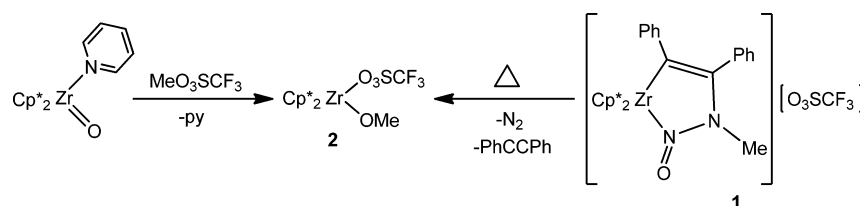
undergoes thermal extrusion of N_2 to generate the oxy-metallacyclobutene complex $\text{Cp}^*_2\text{Zr}(\text{OCPhCPH})$.¹²

The moderate to low yield associated with the preparation of **1** suggested that other products could be formed from this reaction. Accordingly, it was found that the filtrate resulting from the separation of **1** contained another Zr(IV) material, namely, the alkoxide complex $\text{Cp}^*_2\text{Zr}(\text{OMe})(\text{O}_3\text{SCF}_3)$ (**2**) in 26% yield, subsequent to recrystallization from pentane at -35°C (Scheme 3). The low isolated yield of the substance can be attributed to its high lipophilicity in most common organic solvents, including pentane and hexane, in addition to complex **1** being the major product. Compound **2** displays ^1H NMR spectral resonances consistent with two equivalent Cp^* rings (1.80 ppm), and a downfield singlet shift, which is diagnostic of a methoxide ligand (4.03 ppm). In addition, formation of a triflate complex was evidenced by a singlet at -78.7 ppm in the ^{19}F NMR spectrum. Intuitively, the high solubility of **2** in most common organic solvents suggests the triflate anion to be coordinating to the coordinatively unsaturated zirconium(IV) center, especially when similar $\text{Cp}^*_2\text{Zr}(\text{OR})(\text{X})$ ($\text{R} = \text{SiMe}_3$, $\text{X} = \text{Cl}$; $\text{R} = \text{Me}$, $\text{X} = \text{I}$) have been reported.^{15c,48} To substantiate the connectivity of **2**, an independent and more convenient route to its formation was undertaken. It was found that complex **2** could be prepared in quantitative yield by alkylation of Parkin's terminal oxo species $\text{Cp}^*_2\text{Zr}(\text{O})(\text{NC}_3\text{H}_5)$ ^{15c} with MeO_3SCF_3 (Scheme 4).⁴⁸

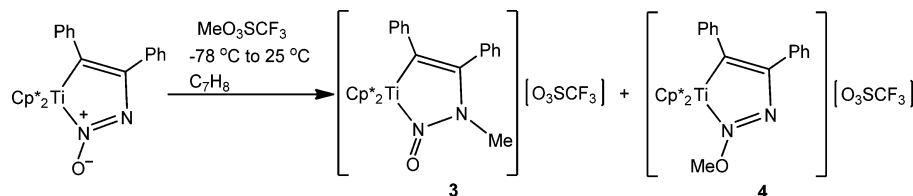
The formation of **2** from the alkylation of metastable $\text{Cp}^*_2\text{Zr}(\text{N}(\text{O})\text{NCPHCPH})$ suggested that **1**, or the byproduct resulting from N_2 extrusion in $\text{Cp}^*_2\text{Zr}(\text{N}(\text{O})\text{NCPHCPH})$, $\text{Cp}^*_2\text{Zr}(\text{OCPhCPH})$, could be reacting with MeO_3SCF_3 . It was observed by ^1H NMR spectroscopy that complex **1** slowly decays in solution at -35°C (several days) to afford a complicated mixture of products, one of which was indeed **2**. In fact, thermolysis of complex **1** in chlorobenzene affords **2** and toluene among many other byproducts, but isolation of any zirconium complexes from the reaction mixture was hampered by their high solubility as well as their formation in low yield (Scheme 4). Independently, it was found that $\text{Cp}^*_2\text{Zr}(\text{OCPhCPH})$ does not react with MeO_3SCF_3 under similar conditions to form **1**, therefore suggesting that **2** is most likely formed from the decomposition of **1**. A less likely pathway might involve alkylation of $\text{Cp}^*_2\text{Zr}(\eta^2\text{-PhCCPh})$ preceding N_2O insertion. We also argue against this pathway since MeO_3SCF_3 does not react with the diphenylacetylene complex under similar conditions. Instead, we propose that complex **2** is likely formed from alkylation at the β -nitrogen to form **1**, followed by migration to the β -oxygen, which then undergoes a series of steps including ring expansion as well as N_2 and toluene elimination by retrocycloadditions. Another process could be a concerted addition of the methyl cation directly to the β -O atom of $\text{Cp}^*_2\text{Zr}(\text{N}(\text{O})\text{NCPHCPH})$ (without going through **1**), followed by analogous transformation steps such as ring expansion as well as N_2 and toluene elimination or retrocycloaddition. Regardless, methyl alkylation at the β -N intuitively implies complex **1** to be a kinetic product. The hypothesis of whether alkylation takes place at the β -oxygen or β -nitrogen was further investigated by using a more stable analogue of **1**, namely, the complex $\text{Cp}^*_2\text{Ti}(\text{N}(\text{O})\text{NCPHCPH})$, prepared analogously from the reaction of $\text{Cp}^*_2\text{Ti}(\eta^2\text{-PhCPh})$ with N_2O .¹¹

Alkylation of $\text{Cp}^*_2\text{Ti}(\text{N}(\text{O})\text{NCPHCPH})$ with MeOTf . When a toluene solution of $\text{Cp}^*_2\text{Ti}(\text{N}(\text{O})\text{NCPHCPH})$ was treated with one equivalent of MeO_3SCF_3 at -78°C , an

Scheme 4. Independent Syntheses of **2** by Reaction of the Terminal Oxo $\text{Cp}^*_2\text{Zr}(\text{O})(\text{py})$ with MeO_3SCF_3 or via Thermolysis of **1**



Scheme 5. Alkylation of the Azoxymetallacyclobutene Complex $\text{Cp}^*_2\text{Ti}(\text{N}(\text{O})\text{NCPhCPh})$ with MeO_3SCF_3 to Form an Equal Mixture of **3** and **4**



immediate precipitation of a brown oil was observed. Decanting the solution and extraction of the oil with CH_2Cl_2 followed by layering with Et_2O afforded dark maroon single crystals of a mixture of two salts, $[\text{Cp}^*_2\text{Ti}(\text{N}(\text{OMe})\text{NCPhCPh})][\text{O}_3\text{SCF}_3]$ (**3**) and $[\text{Cp}^*_2\text{Ti}(\text{N}(\text{O})\text{N}(\text{Me})\text{CPhCPh})][\text{O}_3\text{SCF}_3]$ (**4**), in 68% combined isolated yield (Scheme 5). The ^1H NMR spectrum of the salts revealed a nearly 1:1 ratio of compounds with characteristic resonances for the methyl protons on the Cp^* rings as well as multiplets for a total of four different phenyl environments (two per complex). The most definitive evidence for formation of two complexes was the observation of two singlets residing at 3.93 (*O*-methyl moiety in **4**) and 3.36 (*N*-methyl moiety in **3**) ppm. We tentatively assign the latter resonances on the basis of electron-withdrawing effects of *O* vs *N* as well as comparison with the observed resonance for the *N*-bound methyl analogue, **1** (*vide supra*, 4.03 ppm). In addition, the ^{13}C NMR spectrum corroborates formation of a mixture of salts via the observation of two distinct $\text{Ti}-\text{C}$ resonances at 225.8 and 204.3 ppm, as well as the methyl carbon resonances (formally from Me^+ in MeOTf) at 60.0 and 37.2 ppm, respectively.

Single-crystal X-ray diffraction studies revealed not only that both **4** and **5** cocrystallize (one molecule per asymmetric unit) but that the methyl group is both observed at the β -*O* and β -*N* with nearly half-occupancies (Figure 2). Although our

molecular structure (and NMR spectroscopy) provides concrete evidence for methylation taking place at both the β -*O* and β -*N*, the metrical parameters about the $\text{Cp}^*_2\text{Ti}(\text{N}(\text{O})\text{NCPhCPh})$ scaffold represent the average of the two systems, therefore limiting our discussion of resonances from the metrical parameters (Table 3 lists selected metrical parameters

Table 3. Selected Bond Lengths (Å) for Complexes $\text{Cp}^*_2\text{Ti}(\text{N}(\text{O})\text{NCPhCPh})$ and **5**

	$\text{Cp}^*_2\text{Ti}(\text{N}(\text{O})\text{NCPhCPh})^{11}$	3/4	5
Ti–N(1)	2.088(4)	2.132(3)	2.185(4)
Ti–C(31)	2.210(5)	2.187(3)	2.208(5)
N(1)–N(2)	1.294(7)	1.270(4)	1.279(5)
N(1)–O(1)	1.281(6)	1.321(3)	1.295(5)
N(2)–C(41)	1.435(7)	1.441(4)	1.430(6)
C(31)–C(41)	1.344(7)	1.357(4)	1.349(7)
O(1)C(1B)	n/a	1.647(8)	n/a
N(2)C(1A)	n/a	1.449(6)	n/a

for the average of the core structures of **3** and **4** and comparison to the neutral species $\text{Cp}^*_2\text{Ti}(\text{N}(\text{O})\text{NCPhCPh})$.¹¹ As anticipated, multiple attempts to separate complexes **3** from **4** were hindered by their similar solubilities.

Synthesis of the Ti(III) Radical Anion Salt $[\text{K}(\text{2,2,2-Kryptofix})][\text{Cp}^*_2\text{Ti}(\text{N}(\text{O})\text{NCPhCPh})]$ (6**) and Theoretical Analysis of the Azoxytitanacyclobutene Fragment.** Our studies have demonstrated that the “ $\text{N}(\text{O})\text{N}$ ” moiety (derived from N_2O) in systems of the type $\text{Cp}^*_2\text{M}(\text{N}(\text{O})\text{NCPhCPh})$ ($\text{M} = \text{Zr}$ and Ti) can be further functionalized with an electrophile to form a metal-bound dialkylnitrosoamine, and in the case of titanium, the *O*-methylated regioisomer can be obtained as a mixture with the *N*-methylated product. Having studied the reactivity of complexed nitrous oxide with an electrophile, we inquired if the azoxymetallacyclobutene motif would be stable to reducing conditions. Since N_2O is by itself a thermodynamically powerful oxidant, one would anticipate systems such as $\text{Cp}^*_2\text{M}(\text{N}(\text{O})\text{NCPhCPh})$ to also be good oxidants. Accordingly, complex $\text{Cp}^*_2\text{Ti}(\text{N}(\text{O})\text{NCPhCPh})$ was examined by cyclic voltammetry to reveal an irreversible one-electron anodic event at 0.30 V (vs $\text{FcCp}_2^{+/0}$ referenced at 0.0 V). A cathodic scan showed a reversible one-electron process

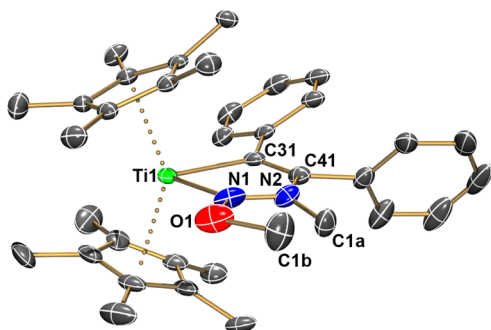
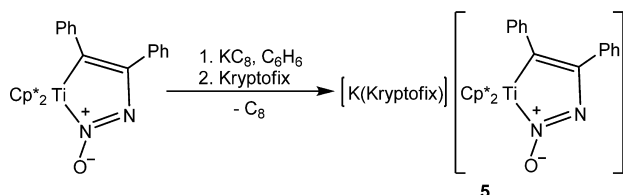


Figure 2. Perspective view of the molecular structure of the cationic component for a cocrystal for the average of complexes **3** and **4**, depicting the atom-labeling ellipsoid plot at the 50% probability level. Both β -*N* and β -*O* methyl alkylated sites are shown.

centered at -1.80 V, thus implying that complex $\text{Cp}^*_2\text{Ti}(\text{N}(\text{O})\text{NCPPhCPh})$ is not a good oxidant given such a highly negative potential. Chemical reduction of $\text{Cp}^*_2\text{Ti}(\text{N}(\text{O})\text{NCPPhCPh})$ with one equivalent of KC_8 in benzene afforded an extremely air-sensitive green solution, from which the Ti(III) radical anion $[\text{K}(2,2,2\text{-Kryptofix})][\text{Cp}^*_2\text{Ti}(\text{N}(\text{O})\text{NCPPhCPh})]$ (**5**) has been isolated as an encrypted dark green crystalline material in 68% yield (Scheme 6).

Scheme 6. Reduction of $\text{Cp}^*_2\text{Ti}(\text{N}(\text{O})\text{NCPPhCPh})$ with KC_8 to Form the Ti(III) Complex Salt **5**^a



^aH atoms have been omitted for clarity purposes.

Complex **5** is paramagnetic, therefore displaying only a couple of extremely broad resonances in the ^1H NMR spectrum (2.20 and 7.50 ppm), while relatively sharp resonances for the cryptand cationic portion (1.95, 2.73, and 3.70 ppm) are clearly visible. At room temperature, a solution magnetic moment measurement of complex **5** in THF solution was consistent with this complex having one unpaired electron ($\mu_{\text{eff}} = 2.28 \mu_{\text{B}}$, Evans' method). In addition, the room-temperature X-band EPR spectrum of **5** in THF revealed the unpaired electron to reside primarily on titanium ($g_{\text{iso}} = 1.9846$) with $A_{\text{iso}} = 8.55$ G (^{47}Ti , $I = 5/2$, 7.4%; ^{47}Ti , $I = 7/2$, 5.4%), in addition to some superhyperfine coupling to the $\alpha\text{-N}$ with $A_{\text{iso}} = 2.0$ G (^{14}N , $I = 1$, 99.64%), and coupling to the more distant $\beta\text{-N}$ ($A_{\text{iso}} = 0.5$ G, ^{14}N , $I = 1$, 99.64%) composing the azoxymetallacycle ring (Figure 3). Although the coupling constant of the unpaired electron with titanium is characteristic for $\text{Cp}^*_2\text{Ti}(\text{III})\text{L}$ or $\text{Cp}^*_2\text{V}(\text{IV})\text{L}_2$ ($\text{Cp}^* = \text{C}_5\text{H}_5$ or $\text{C}_5\text{H}_4\text{Me}$) systems studied previously,^{49,50} complex **5** represents the first example of a stable transition metal radical species derived from N_2O complexation. Unfortunately, multiple attempts to prepare the

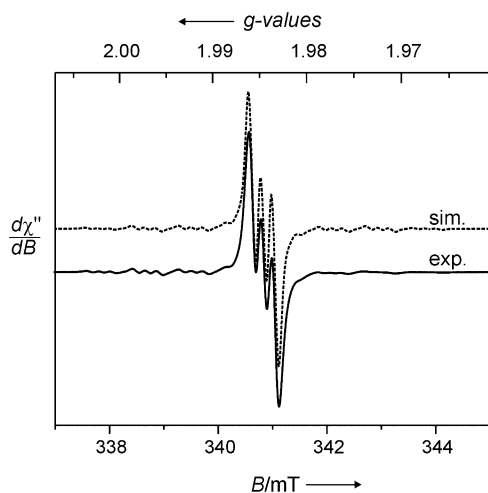


Figure 3. X-band EPR spectrum of complex **5**, recorded in THF solution at 298 K. The simulated spectrum (sim.) is shown above the experimental spectrum (exp.).

zirconium analogue of **5** were unsuccessful, even when performing the reaction at -78 °C and in the presence of cryptand as a trap.⁵¹

Single crystals of **5** reveal a discrete salt with an essentially intact azoxymetallacyclobutene ligand, grossly similar to that of its precursor $\text{Cp}^*_2\text{Ti}(\text{N}(\text{O})\text{NCPPhCPh})$.¹¹ The only significant perturbation is the Ti–N(1) bond distance of 2.185(4) Å, which reflects slight elongation from that of its neutral counterpart (Figure 4). Table 2 lists selected metrical

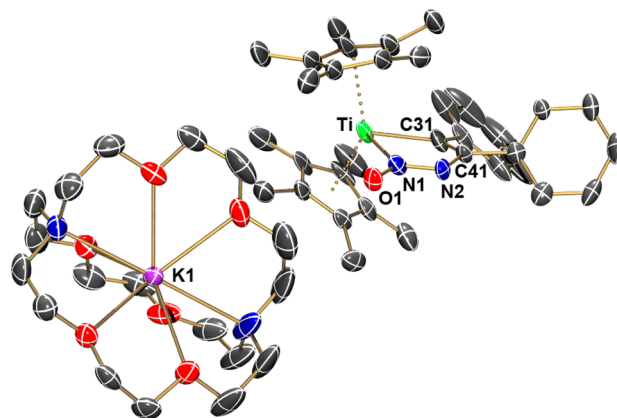


Figure 4. Perspective view of the molecular structure of complex **5**, showing the atom-labeling ellipsoid plot at the 50% probability level. H atoms and a THF confined in the asymmetric unit have been omitted for clarity.

parameters for $\text{Cp}^*_2\text{Ti}(\text{N}(\text{O})\text{NCPPhCPh})$ ¹¹ and the radical anion core of **5**. Intuitively, inclusion of an unpaired electron should not deform the core structure in $\text{Cp}^*_2\text{Ti}(\text{N}(\text{O})\text{NCPPhCPh})$, but only permute the Ti–N distance slightly, since the orbital housing the unpaired electron should be a nonbonding metal d orbital. Surprisingly though, the N–O and N–N distances are relatively unperturbed when compared to $\text{Cp}^*_2\text{Ti}(\text{N}(\text{O})\text{NCPPhCPh})$, even though the X-band EPR spectrum implies some delocalization of the unpaired electron onto these sites.

In order to understand the chemistry of the azoxymetallacyclobutene moiety toward electrophiles or reductants, we relied on theoretical studies using the Gaussian 09 package⁴⁴ at the B3PW91 level of theory to dissect the molecular picture of the complexes $\text{Cp}^*_2\text{M}(\text{N}(\text{O})\text{NCPPhCPh})$ ($\text{M} = \text{Ti}$ and Zr). When inspecting the molecular representation of the simplified models of $\text{Cp}^*_2\text{M}(\text{N}(\text{O})\text{NCPPhCPh})$, namely, $\text{Cp}_2\text{M}(\text{N}(\text{O})\text{NCMeCMe})$, it can be observed how the azoxymetallacyclobutene moiety dominates the frontier orbital picture. For example, the HOMOs for each metal complex are nearly identical and expose the $\text{N}=\text{N}$ π -bond, which is out of phase with the $\beta\text{-O}$ atom (Figure 5), and thus consistent with resonance structures A or C depicted in Scheme 2 (*vide supra*). From the HOMO, the most obviously exposed nucleophilic sites are the $\beta\text{-N}$ and $\beta\text{-O}$. This pattern well explains why Me^+ addition occurs at both the $\beta\text{-N}$ and $\beta\text{-O}$ for $\text{M} = \text{Ti}$. However, it does not explain why alkylation occurs only (based on our observations) at the $\beta\text{-N}$ for $\text{M} = \text{Zr}$. In fact, close inspection of the orbital populations for each individual atom do not reflect any notable discrepancies in the atomic contributions from the $\beta\text{-N}$ and $\beta\text{-O}$ atoms. For $\text{M} = \text{Ti}$, the LUMO and LUMO+1 illustrate a titanium $d(x^2-y^2)$ orbital that interacts in a “slipped” σ fashion with the $\alpha\text{-N}$. In contrast to the HOMO orbitals, the

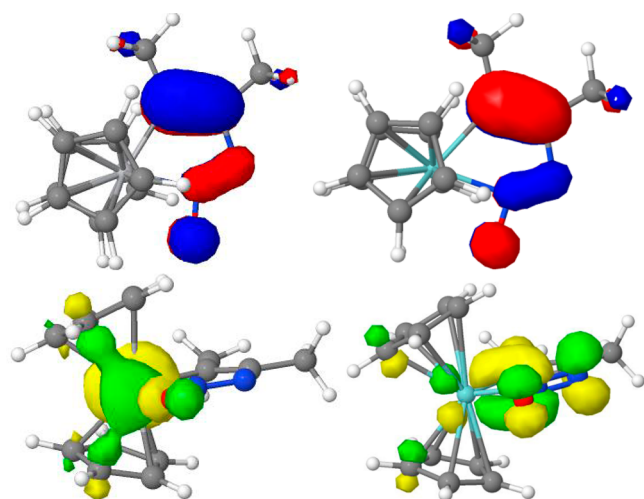


Figure 5. Most important frontier orbitals computed for the complexes $\text{Cp}^*_2\text{M}(\text{N}(\text{O})\text{NCPHCPh})$. Shown are the HOMO (top left) and LUMO (bottom left) for $\text{M} = \text{Ti}$, and HOMO (top right) and LUMO (bottom right) for $\text{M} = \text{Zr}$. The initial geometry of $\text{Cp}_2\text{Ti}(\text{N}(\text{O})\text{NCMeCMe})$ and $\text{Cp}_2\text{Zr}(\text{N}(\text{O})\text{NCMeCMe})$ was adapted from a refined crystal structure of $\text{Cp}^*_2\text{Ti}(\text{N}(\text{O})\text{NCPHCPh})$,¹¹ where all methyl groups on the Cp^* have been replaced with H and phenyl groups on the metallacycle have been replaced with methyls.

LUMO of $\text{Cp}_2\text{Zr}(\text{N}(\text{O})\text{NCMeCMe})$ shows a π -like d orbital of Zr having an in-phase combination with the β -N but where this is significantly more delocalized about the azoxymetallacyclobutene moiety (Figure 5). This might explain why chemical reduction of $\text{Cp}^*_2\text{Zr}(\text{N}(\text{O})\text{NCPHCPh})$ is not clean since the LUMO is not just an empty d orbital. In fact, the LUMO+1 for $\text{Cp}_2\text{Zr}(\text{N}(\text{O})\text{NCMeCMe})$ has more similarities to the LUMO observed in $\text{Cp}_2\text{Ti}(\text{N}(\text{O})\text{NCMeCMe})$, which shows a hybridized nonbonding metal-based orbital with mostly $d(x^2-y^2)$ character (Figure 5). Petersen and Dahl have described similar d^1 bent metallocenes of vanadium, namely, $\text{Cp}'_2\text{VL}_2(4+)$, and have suggested the unpaired electron to reside primarily on a vanadium a_1 -type MO mainly composed of $d(z^2)$, but augmented with some $d(x^2-y^2)$.⁵⁰ Due to the minor structural differences observed between $\text{Cp}^*_2\text{Ti}(\text{N}(\text{O})\text{NCPHCPh})$ and the $\text{Ti}(\text{III})$ derivative $[\text{Cp}^*_2\text{Ti}(\text{N}(\text{O})\text{NCPHCPh})]^-$ (*vide supra*), the above results suggest the unpaired electron to virtually reside in a weakly bonding wedge orbital (or nonbonding SOMO), which should slightly reduce the bond order of the Ti and α -N, but also the $\text{N}=\text{N}$ π - and $\text{N}-\text{O}$ interaction. The nonbonding nature of the SOMO is not surprising, since attempts to alkylate complex **5** with various electrophiles resulted in clean oxidation to $\text{Cp}^*_2\text{Ti}(\text{N}(\text{O})\text{NCPHCPh})$ rather than further functionalization. As a result, the frontier orbitals predicted by theoretical methods explain the mode of reactivity observed with $\text{Cp}^*_2\text{Ti}(\text{N}(\text{O})\text{NCPHCPh})$ well and corroborate our structural and spectroscopic findings for its radical anion, $[\text{Cp}^*_2\text{Ti}(\text{N}(\text{O})\text{NCPHCPh})]^-$. Unfortunately, we are uncertain as to why Me^+ does not alkylate the β -O site (or why this species is not observed) of $\text{Cp}^*_2\text{Zr}(\text{N}(\text{O})\text{NCPHCPh})$, but we do propose that the Me^+ does migrate to the β -O, resulting in degradation of the metallacycle.

CONCLUSIONS

In this work, we have shown that metal coordination of nitrous oxide forms an azoxymetallacycle complex of the type $\text{Cp}^*_2\text{M}(\text{N}(\text{O})\text{NCPHCPh})$ ($\text{M} = \text{Ti}$ and Zr), in which the

activated N_2O is further functionalized at both the β -O and β -N moieties. At this end, the apparent variation in reactivity of the electrophile with each azoxymetallacycle remains unclear. However, we suggest that the observed divergent reactivity is due to the $\text{Zr}-\text{O}$ versus $\text{Ti}-\text{O}$ bond strengths and relates to the thermodynamic stability of the titanium azoxymetallacycle precursor complex relative to that of zirconium, which spontaneously extrudes N_2 to yield the oxymetallacyclobutene complex. Using $\text{Cp}^*_2\text{Ti}(\text{N}(\text{O})\text{NCPHCPh})$ however, we are able to trap the *O*-methylated intermediate, resulting in N_2 and toluene extrusion in the case of Zr . The regioselectivity for Me^+ addition suggests the HOMO in $\text{Cp}^*_2\text{M}(\text{N}(\text{O})\text{NCPHCPh})$ to be predominantly dominated by the lone pairs in the β -O and β -N positions. In contrast, the LUMO for $\text{M} = \text{Ti}$ represents a slipped nonbonding metal-based σ orbital. This feature contrasts $\text{M} = \text{Zr}$, where there is more azoxymetallacycle character in the LUMO. Despite our shortcoming to use N_2O as a catalytic O atom transfer source, complexes of the type $\text{Cp}^*_2\text{M}(\text{N}(\text{O})\text{NCPHCPh})$ represent attractive synthetic targets since N_2O can be a reagent for the preparation of the nitrosimine functionality, which can be further functionalized with Me^+ to a dialkyl nitrosamine. Given the fact that N_2O binding to metal complexes has been predicted and shown to occur preferentially at the terminal nitrogen atom,^{24b,52} other systems can potentially harness the oxidizing power of this resourceful, but underutilized reagent.

ASSOCIATED CONTENT

Supporting Information

CIF files for the structures of compounds **1**, **3/4**, and **5**. This material is available free of charge via the Internet at <http://pubs.acs.org>.

AUTHOR INFORMATION

Corresponding Author

*E-mail: mindiola@sas.upenn.edu.

Present Addresses

[†]Department of Chemistry, University of Pennsylvania, Philadelphia, PA 19104, USA.

[‡]Department of Chemistry, Earlham College, Richmond, IN 47374, USA.

[§]Department of Chemistry and Pharmacy, Inorganic Chemistry, Friedrich-Alexander University Erlangen-Nürnberg (FAU), 91058 Erlangen, Germany.

Notes

The authors declare no competing financial interest.

¹Deceased March 6, 2014.

ACKNOWLEDGMENTS

This paper is dedicated to the memory of Prof. Gregory L. Hillhouse, a terrific chemist, advisor, and beloved friend. In order to pay our last respects to a great and unique scientist, we voice both mentally and physically that a sad day has come, one where we wish a fond farewell to a wonderful man, a man whom we were all so very privileged to have known and worked with. We thank the National Science Foundation for financial support, Professor M. D. Hopkins and Dr. Daniel E. Haines for access to a BAS potentiostat and software, and Dr. Ian Steele for some assistance with X-ray crystallography. D.J.M. acknowledges postdoctoral fellowship support from the Ford Foundation and the National Institutes of Health.

REFERENCES

- (1) (a) Trogler, W. C. *Coord. Chem. Rev.* **1999**, *187*, 303. (b) Bottomley, F. *Polyhedron* **1992**, *11*, 1707. (c) Parmon, V. N.; Panova, G. I.; Uriarte, A.; Noskova, A. S. *Catal. Today* **2005**, *100*, 115.
- (2) Holm, R. H. *Chem. Rev.* **1987**, *87*, 1401.
- (3) Bottomley, F.; Sutin, L. *Adv. Organomet. Chem.* **1988**, *28*, 339.
- (4) Bottomley, F.; Brintzinger, H. *J. Chem. Soc., Chem. Commun.* **1978**, 234.
- (5) Bottomley, F.; Lin, I. J. B.; White, P. S. *J. Am. Chem. Soc.* **1981**, *103*, 703.
- (6) Bottomley, F.; Egharevba, G. O.; Lin, I. J. B.; White, P. S. *Organometallics* **1985**, *4*, 550.
- (7) Bottomley, F.; Lin, I. J. B.; Mukaida, M. *J. Am. Chem. Soc.* **1980**, *102*, 5238.
- (8) (a) Bottomley, F.; Drummond, D. F.; Paez, D. E.; White, P. S. *J. Chem. Soc., Chem. Commun.* **1986**, 1752. (b) Berg, D. J.; Burns, C. J.; Andersen, R. A.; Zalkin, A. *Organometallics* **1989**, *8*, 1865.
- (9) Vaughan, G. A.; Rupert, P. B.; Hillhouse, G. L. *J. Am. Chem. Soc.* **1987**, *109*, 5538.
- (10) Vaughan, G. A.; Hillhouse, G. L.; Lum, R. T.; Buchwald, S. L.; Rheingold, A. L. *J. Am. Chem. Soc.* **1988**, *110*, 7215.
- (11) Vaughan, G. A.; Sofield, C. D.; Hillhouse, G. L.; Rheingold, A. L. *J. Am. Chem. Soc.* **1989**, *111*, 5491.
- (12) Vaughan, G. A.; Hillhouse, G. L.; Rheingold, A. L. *J. Am. Chem. Soc.* **1990**, *112*, 7994.
- (13) Matsunaga, P. T.; Hillhouse, G. L.; Rheingold, A. L. *J. Am. Chem. Soc.* **1993**, *115*, 2075.
- (14) Matsunaga, P. T.; Mavropoulos, J. C.; Hillhouse, G. L. *Polyhedron* **1995**, *14*, 175.
- (15) (a) McNeill, K.; Bergman, R. G. *J. Am. Chem. Soc.* **1999**, *121*, 8260 and references therein. (b) Smith, M. R.; Matsunaga, P. T.; Andersen, R. A. *J. Am. Chem. Soc.* **1993**, *115*, 7049. (c) Howard, W. A.; Trnka, T. M.; Waters, M.; Parkin, G. *J. Organomet. Chem.* **1997**, *528*, 95 and references therein. (d) Kaplan, A. W.; Bergman, R. G. *Organometallics* **1998**, *17*, 5072.
- (16) Groves, J. T.; Roman, J. S. *J. Am. Chem. Soc.* **1995**, *117*, 5594 and references therein.
- (17) The dinitrogen complex $[\text{HCo}(\text{N}_2)(\text{PPh}_3)_3]$ as the catalyst precursor remains one of the only well-characterized homogeneous and catalytic oxidation reactions of N_2O : Yamamoto, A.; Kitazume, S.; Pu, L. S.; Ikeda, S. *J. Am. Chem. Soc.* **1971**, *93*, 371.
- (18) (a) Otten, E.; Neu, R. C.; Stephan, D. W. *J. Am. Chem. Soc.* **2009**, *131*, 9918. (b) Neu, R. C.; Otten, E.; Lough, A.; Stephan, D. W. *Chem. Sci.* **2011**, *2*, 170.
- (19) Harman, W. H.; Chang, C. J. *J. Am. Chem. Soc.* **2007**, *129*, 15128.
- (20) (a) Banks, R. G. S.; Henderson, R. J.; Pratt, J. M. *Chem. Commun.* **1967**, 387. (b) Banks, R. G. S.; Henderson, R. J.; Pratt, J. M. *J. Chem. Soc. (A)* **1968**, 2886.
- (21) Bottomley, F.; Lin, I. J. B.; Mukaida, M. *J. Am. Chem. Soc.* **1980**, *102*, 5238.
- (22) (a) Armor, J. N.; Taube, H. *J. Am. Chem. Soc.* **1971**, *93*, 6476. (b) Armor, J. N.; Taube, H. *J. Am. Chem. Soc.* **1969**, *91*, 6874.
- (23) (a) Armor, J. N.; Taube, H. *J. Am. Chem. Soc.* **1970**, *92*, 2560. (b) Piro, N. A.; Lichterman, M. F.; Hill Harman, W.; Chang, C. J. *J. Am. Chem. Soc.* **2011**, *133*, 2108. (c) Tskhovrebov, A. G.; Solari, E.; Wodrich, M. D.; Scopelliti, R.; Severin, K. *Angew. Chem., Int. Ed.* **2011**, *51*, 232. (d) Neu, R. C.; Otten, E.; Lough, A.; Stephan, D. W. *Chem. Sci.* **2011**, *2*, 170. (e) Ménard, G.; Hatnean, J. A.; Cowley, H. J.; Lough, A. J.; Rawson, J. M.; Stephan, D. W. *J. Am. Chem. Soc.* **2013**, *135*, 6446.
- (24) (a) Armor, J. N.; Taube, H. *Chem. Commun.* **1971**, 287.
- (25) Bottomley, F.; Crawford, J. R. *J. Am. Chem. Soc.* **1972**, *94*, 9092.
- (26) Bottomley, F.; Brooks, W. V. *Inorg. Chem.* **1977**, *16*, 501.
- (27) Pamplin, C. B.; Ma, E. S. F.; Safari, N.; Rettig, S. J.; James, B. R. *J. Am. Chem. Soc.* **2001**, *123*, 8596.
- (28) An N_2O adduct has been proposed but not isolated. (a) McCarthy, M. R.; Crevier, T. J.; Bennett, B.; Dehestani, A.; Mayer, J. M. *J. Am. Chem. Soc.* **2000**, *122*, 12391. (b) Lee, J. H.; Pink, M.; Tomaszewski, J.; Fan, H.; Caulton, K. G. *J. Am. Chem. Soc.* **2007**, *129*, 8706.
- (29) Labahn, T.; Mandel, A.; Magull, J. Z. *Anorg. Allg. Chem.* **1999**, *625*, 1273.
- (30) For some examples of terminal metal oxo formation using N_2O as the O atom source: (a) Antonelli, D. M.; Schaefer, W. P.; Parkin, G.; Bercaw, J. E. *J. Organomet. Chem.* **1993**, *462*, 213. (b) Howard, W. A.; Waters, M.; Parkin, G. *J. Am. Chem. Soc.* **1993**, *115*, 4917. (c) Howard, W. A.; Parkin, G. *J. Am. Chem. Soc.* **1994**, *116*, 606. (d) Kilgore, U. J.; Sengelaub, C. A.; Fan, H.; Tomaszewski, J.; Pink, M.; Karty, J. A.; Baik, M.-H.; Mindiola, D. J. *Organometallics* **2009**, *28*, 843. (e) Cummins, C. C.; Schrock, R. R.; Davis, W. M. *Inorg. Chem.* **1994**, *33*, 1448. (f) Kisko, J. L.; Hascall, T.; Parkin, G. *J. Am. Chem. Soc.* **1997**, *119*, 7609. (g) Crestani, M. G.; Hickey, A.; Pinter, B.; Cavaliere, V. N.; Gao, X.; Ito, J.-i.; Chen, C.-H.; Mindiola, D. J. *J. Am. Chem. Soc.* **2013**, *135*, 14754. (h) Crestani, M. G.; Pinter, B.; Olsz, A.; Bailey, B. C.; Fortier, S.; Gao, X.; Chen, C.-H.; Baik, M.-H.; Mindiola, D. J. *Chem. Sci.* **2013**, *4*, 2543. (i) Cavaliere, V. N.; Crestani, M. G.; Pinter, B.; Chen, C.-H.; Pink, M.; Baik, M.-H.; Mindiola, D. J. *J. Am. Chem. Soc.* **2011**, *133*, 10700. (j) Andino, J. G.; Kilgore, U. J.; Ozarowski, A.; Krzystek, J.; Telser, J.; Pink, M.; Baik, M.-H.; Mindiola, D. J. *Chem. Sci.* **2010**, *1*, 351.
- (31) Examples in which nitrous oxide oxidizes the metal center without N_2 extrusion and rupture of the N–N bond have been reported. (a) Laplaza, C. E.; Odom, A. L.; Davis, W. M.; Cummins, C. C.; Protasiewicz, J. D. *J. Am. Chem. Soc.* **1995**, *117*, 4999. (b) Johnson, A. R.; Davis, W. M.; Cummins, C. C.; Serron, S.; Nolan, S. P.; Musaev, D. G.; Morokuma, K. *J. Am. Chem. Soc.* **1998**, *120*, 2071. (c) Cherry, J. P. F.; Johnson, A. R.; Baraldo, L. M.; Tsai, Y. C.; Cummins, C. C.; Kryatov, S. V.; Rybak-Akimova, E. V.; Kapps, K. B.; Hoff, C. D.; Haar, C. M.; Nolan, S. P. *J. Am. Chem. Soc.* **2001**, *123*, 7271.
- (32) This rare form of metallacycle is described as an azoxy derivative, with the heteroatomic bond distances being comparable to *p*-azoxyanisole, *p*- $\text{MeOC}_6\text{H}_4\text{N}(\text{O})=\text{NC}_6\text{H}_4$ -*p*- OMe : Krigbaum, W. R.; Chatani, Y.; Barber, P. G. *Acta Crystallogr., Sect. B* **1970**, *26*, 826, 97.
- (33) (a) Tan, S. A.; Grant, R. B.; Lambert, R. M. *J. Catal.* **1987**, *104*, 156. (b) Liu, H.-F.; Liu, R.-S.; Liew, K. Y.; Johnson, R. E.; Lunsford, J. H. *J. Am. Chem. Soc.* **1984**, *106*, 4117.
- (34) (a) Sobolev, V. I.; Kharitonov, A. S.; Paukshtis, Y. A.; Panov, G. I. *J. Mol. Catal.* **1993**, *84*, 117. (b) Ebner, J. R.; Felthouse, T. R.; Fentress, D. C. U.S. Patent 5,874,646, 1996. (c) Panov, G. I.; Uriarte, A. K.; Rodkin, M. A.; Sobolev, V. I. *Catal. Today* **1998**, *41*, 365.
- (35) (a) Liu, H.-F.; Liu, R.-S.; Liew, K. Y.; Johnson, R. E.; Lunsford, J. H. *J. Am. Chem. Soc.* **1984**, *106*, 4117. (b) Liu, R.-S.; Iwamoto, M.; Lunsford, J. H. *J. Chem. Soc., Chem. Commun.* **1982**, 78.
- (36) For a general description of the equipment and techniques used in carrying out this chemistry see: Burger, B. J.; Bercaw, J. E. In *Experimental Organometallic Chemistry*; Wayda, A. L.; Darensbourg, M. Y., Eds.; ACS Symposium Series 357; American Chemical Society: Washington, DC, 1987; pp 79–98.
- (37) Threlkel, R. S. Ph.D. Thesis, California Institute of Technology, 1980.
- (38) Schwindt, M.; Lejon, T.; Hegedus, L. *Organometallics* **1990**, *9*, 2814.
- (39) List, A. K.; Koo, K.; Rheingold, A. L.; Hillhouse, G. L. *Inorg. Chim. Acta* **1997**, *270*, 399.
- (40) Sur, S. K. *J. Magn. Reson.* **1989**, *82*, 169.
- (41) Evans, D. F. *J. Chem. Soc.* **1959**, 2003.
- (42) All software and sources of scattering factors are contained in the SHELXTL program library: Sheldrick, G. *SHELXTL* (version 5.1); Bruker Analytical Systems: Madison, WI.
- (43) Frisch, M. J.; Trucks, G. W.; Schlegel, H. B.; Scuseria, G. E.; Robb, M. A.; Cheeseman, J. R.; Scalmani, G.; Barone, V.; Mennucci, B.; Petersson, G. A.; Nakatsuji, H.; Caricato, M.; Li, X.; Hratchian, H. P.; Izmaylov, A. F.; Bloino, J.; Zheng, G.; Sonnenberg, J. L.; Hada, M.; Ehara, M.; Toyota, K.; Fukuda, R.; Hasegawa, J.; Ishida, M.; Nakajima, T.; Honda, Y.; Kitao, O.; Nakai, H.; Vreven, T.; Montgomery, J. A., Jr.; Peralta, J. E.; Ogliaro, F.; Bearpark, M.; Heyd, J. J.; Brothers, E.; Kudin, K. N.; Staroverov, V. N.; Kobayashi, R.; Normand, J.; Raghavachari, K.

Rendell, A.; Burant, J. C.; Iyengar, S. S.; Tomasi, J.; Cossi, M.; Rega, N.; Millam, N. J.; Klene, M.; Knox, J. E.; Cross, J. B.; Bakken, V.; Adamo, C.; Jaramillo, J.; Gomperts, R.; Stratmann, R. E.; Yazyev, O.; Austin, A. J.; Cammi, R.; Pomelli, C.; Ochterski, J. W.; Martin, R. L.; Morokuma, K.; Zakrzewski, V. G.; Voth, G. A.; Salvador, P.; Dannenberg, J. J.; Dapprich, S.; Daniels, A. D.; Farkas, Ö.; Foresman, J. B.; Ortiz, J. V.; Cioslowski, J.; Fox, D. J. *Gaussian 09*, Revision A.2; Gaussian, Inc.: Wallingford, CT, 2009.a.

(45) (a) Becke, A. D. *Phys. Rev.* **1988**, A38, 3098. Becke, A. D. *J. Chem. Phys.* **1993**, 98, 1372. (b) Becke, A. D. *J. Chem. Phys.* **1993**, 98, 5648. (c) Perdue, J. P.; Wang, Y. *Phys. Rev. B* **1991**, 45, 13244.

(46) Hariharan, P. C.; Pople, J. A. *Theor. Chim. Acta* **1973**, 28, 213.

(47) (a) Hay, P. J.; Wadt, W. R. *J. Chem. Phys.* **1985**, 82, 270. (b) Wadt, W. R.; Hay, P. J. *J. Chem. Phys.* **1985**, 82, 284. (c) Hay, P. J.; Wadt, W. R. *J. Chem. Phys.* **1985**, 82, 299.

(48) Si–H activation reactions using a terminal titanium oxo has been reported: Hanna, T. E.; Lobkovsky, E.; Chirik, P. J. *Inorg. Chem.* **2007**, 46, 2359.

(49) Lukens, W.; Matsunaga, P. T.; Andersen, R. A. *Organometallics* **1998**, 17, 5240.

(50) (a) Petersen, J. L.; Lichtenberger, D. L.; Fenske, R. F.; Dahl, L. F. *J. Am. Chem. Soc.* **1975**, 97, 6433. (b) Petersen, J. L.; Dahl, L. F. *J. Am. Chem. Soc.* **1975**, 97, 6416. (c) Petersen, J. L.; Dahl, L. F. *J. Am. Chem. Soc.* **1975**, 97, 6422.

(51) It was observed that reduction of the metastable complex $\text{Cp}^*_2\text{Zr}(\text{N}(\text{O})\text{NCPhCPh})$ with KC_8 at -78°C resulted in a green solution, which rapidly decayed to a myriad of products even if the reaction was conducted in the presence of 222-Kryptofix at low temperatures.

(52) Tuan, D. F.-T.; Hoffmann, R. *Inorg. Chem.* **1985**, 24, 871.